Additional Algorithms for Sensor Chip Alignment to Blind Datums

Gary B. Hughes, Ph.D.
Senior Systems Engineer
FLIR Systems Inc.
gary.hughes@flir.com

ABSTRACT: Alignment of the sensor focal plane array (FPA) to optical components is a critical design feature. Imaging system designs include reference datums that provide the basis for manufacturing alignment in each sub-assembly. Measurement of *z* and parallelism positioning can be problematic, since the relevant datum features are often beneath the mounting platform and are obscured to the measurement system. General algorithms for determining sensor chip alignment when datum features are inaccessible to the measurement system have been developed [5]. Pre-characterization measurements of datum surfaces are stored for later use during alignment measurement to determine datum locations. The algorithms are useful for post-mounting alignment measurement, and can also be used for active manufacturing alignment. This paper presents additional algorithms that are useful for active alignment, including methods for determining rotation axes on the aligner-bonder system and for determining actuator motions to bring the FPA into alignment with datums. The algorithms have been successfully implemented for ultra-precision, active manufacturing alignment and post-alignment measurement of infrared imaging systems.

INTRODUCTION

For an imaging system, alignment of the Focal Plane Array (FPA) to optical components is a critical design feature. In particular, optics with shallow depth of field require tight control over parallelism alignment of the FPA image plane to the optical axis. Many applications, such as Telescopes and Satellite Imaging Systems, align optics to the FPA during system integration [*e.g.*, 1,2]. Adjustment of FPA alignment at system integration is accomplished with test equipment and precision sources [3]. This process can overcome minor mis-alignments of the FPA to manufacturing datums that may occur when the FPA is bonded to its mounting platform. Nonetheless, minimizing the FPA mounting error is still important, and even more so for systems that do not have the opportunity to align at system integration, *e.g.*, in volume production. Some systems, such as those containing multiple focal planes, are forced to pay more attention to mounting alignment when the FPA is bonded to its platform since there is less opportunity to overcome minor mis-alignments during system integration.

In a manufacturing context, the sensor element (die) of an imaging system is typically mounted onto a platform using fiducial marks on the die and platform as alignment reference points. The mounting operation typically aims to align the two sets of fiducials. However, the true goal of the alignment should be to place the die in such a way as to position the *active elements of the focal plane* in the specified location of the *datum coordinate system*. That is, the active elements should be aligned to the datums. When using the die fiducials as alignment targets, some tolerance is lost when considering the position of the fiducials in relation to the active elements. That is, the active element is not always located at its nominal location with respect to the fiducial marks. A similar tolerance loss is incurred when aligning to a datum surface that is obscured to the alignment measurement system. Some assumptions are typically made regarding the location of a blind datum within the alignment system, *e.g.*, that the datum is parallel to the measurement system *x*-*y* plane.

Novel Optical Systems Design and Optimization IX, edited by José M. Sasian, Mary G. Turner,
Proceedings of SPIE Vol. 6289, 62890K, (2006) · 0277-786X/06/$15 · doi: 10.1117/12.683300

Accurate means are required for determining alignment of the FPA to its mounting platform based on measurements, for example from optical/encoder systems of an aligner-bonder. Modern methods have been established to determine the location of mechanical reference datums from optical measurements [4]. A common problem in this context is how to determine the datum locations on the mounting platform. Especially for parallelism alignment, reference datums are often obscured from the aligner-bonder optics because they are located on the bottom surface of the platform. A set of algorithms has been described for determining the location of alignment datums that are obscured from measurement during FPA mounting [5]. This method relies on pre-characterization measurements of a mounting tool; the measurements are later used to establish the location of datum surfaces when the datums are obscured from the optical measurement system. This approach can be exploited to reduce the tolerance loss typically encountered when aligning fiducials on the die to non-datum features on the mounting platform. Pre-characterization measurements of both the sensor element and mounting platform are made. These measurements, with algorithms in [5], allow the active elements to be aligned directly to the datum coordinate system, even though neither set of features can be measured directly by the alignment system.

As in [5], this paper assumes that the datum planes define a Euclidean coordinate system, and it is with respect to this datum coordinate system that the active elements of the focal plane must be aligned. The spatial relationships between the fiducials and the active elements and datum surfaces are calculated as 'plane transfer values'. These values are scalars that denote the distance from the fiducials to the datum planes and active elements along vectors determined by the fiducial locations (Figure 1). The central idea is that the spatial relationship between the fiducials and datums does not change when the platform or die orientations change. The fixed relationship between fiducials, datums and active elements can be determined by pre-characterization measurements; the fixed relationships can then be utilized to determine datum and active element locations from fiducial measurements during alignment or post-mounting measurement of die placement. Algorithms required for post-mounting measurement are given explicitly in [5]. This paper extends those algorithms for use during active alignment of imaging elements on a sensor die to blind datums on the mounting platform.

Pre-characterization measurements should provide means to determine two spatial relationships: (1) the location of the active elements with respect to the die fiducials; and (2) the location of the (blind) datum coordinate system with respect to features (often fiducials placed on a mounting tool) that will be accessible to the aligner-bonder measurement system during alignment. These two requirements are first considered separately, then combined to provide a seamless method for active FPA alignment.

DIE PRE-CHARACTERIZATION

Hybridization slip and gap measurements can be utilized to provide plane transfer values from the die fiducials to the probable locations of the active elements. Slip and gap data are typically recorded for feedback to the hybridization process, but these values can also be useful to the FPA alignment process. The alignment operation often aims to place the FPA so that Pixel (1, 1) is at a specified (x, y, z) location within the datum coordinate system established by mechanical datums in the mounting platform. For clocking alignment, the (x, y, z) location of Pixel (1, n) is also required. For parallelism alignment, the (x, y, z) location of Pixel (m, n) is also required. A common approach to alignment uses the nominal locations of Pixel (1, 1), Pixel (1, n) and Pixel (m, n) as 'reference pixels'. The uncertainty of the reference pixel locations in the hybridized FPA is typically

established by the maximum allowable hybridization slip with maximum allowable hybridization gap wedge. This uncertainty could be reduced for the FPA alignment process by using hybridization slip and gap data to estimate the (*x, y, z*) locations of all reference pixels after hybridization.

It is possible to estimate the (*x, y, z*) locations of reference pixels after hybridization using hybridization slip and gap data, along with algorithms from [5]. These measurements provide important feedback to the hybridization process, but they can also be used to improve the FPA alignment process. Figure 2 illustrates the transformations that are used to determine the slipped location of reference pixels. For FPA alignment, the hybridization slip is characterized as the movement of the Detector relative to the Read-Out Integrated Circuit (ROIC) where the FPA fiducials are located. The relative motions are applied to the nominal locations of the detector and ROIC targets to give the absolute positions of the slipped detector targets in the ROIC coordinate system. The hybrid slip values are not always self-consistent; any inconsistencies can be averaged by determining the detector target midpoint after hybridization. If the hybridization slip measurements at both sets of targets give the same *x*- and *y*-values, then only a translation in *x* and *y* (Δx, Δy) is required to describe the offset of the detector with respect to the ROIC. However, if any of the *x*- or *y*-values differ between the two sets of targets, then a translation (Δx, Δy) and a rotation (through some angle θ about some rotation center (x_c, y_c)) is required to describe the offset. For example, suppose that three of the four hybridization slip measurements were zero, and the fourth was 3 microns. There is no single translation (Δx, Δy) that could account for these measurements. A rotation is required. The 'probable' hybridization slip movements can be summarized by a translation (Δx, Δy) and a rotation through an angle θ about the midpoint of the line segment joining the detector targets. The 'probable' resulting position of Pixel (1, 1) is estimated by applying the translation and rotation to the nominal location of Pixel (1, 1) in the ROIC coordinate system. Use of the midpoint for slip calculations provides a 'best-fit' approximation to account for the observed slips. Hybrid gap measurements are then used to determine the plane equation of the bottom of the detector. The *x*-*y* location of Pixel (1, 1) and the image plane equation (from hybrid gap measurements) can then be used to determine the most probable (*x, y, z*) location of Pixel (1, 1).

Some care must be made when interpreting hybridization slip and gap data. The values are recorded in local coordinate systems, and translation to the ROIC coordinate system is critical. The example in Figure 1 shows measurements of individual Detector Slip at targets near ROIC F2 and ROIC F4. These values can be used to determine individual hybridization slip values in ROIC fiducial coordinates:

(x, y) slip of Detector target near ROIC F2 after hybridization:

$$\left(x_{ROIC_{target\,F2}} + x_2,\ \ y_{ROIC_{target\,F2}} + y_2\right) = \left(x_{nom} + x_2,\ \ y_{\mathrm{nom}} + y_2\right)$$

(x, y) slip of Detector target near ROIC F4 after hybridization:

$$\left(x_{ROIC_{target\,F4}} + x_4,\ \ y_{ROIC_{target\,F4}} + y_4\right) = \left(x_{nom} + x_4,\ \ y_{\mathrm{nom}} + y_4\right)$$

From the midpoint formula, and the locations of the individual slipped detector targets, the probable location of the detector target midpoint after hybridization is given by:

$$\left(\frac{x_{ROIC_{target\,F2}} + x_{ROIC_{target\,F4}} + x_2 + x_4}{2}, \frac{y_{ROIC_{target\,F2}} + y_{ROIC_{target\,F4}} + y_2 + y_4}{2}\right)$$

The difference between the nominal midpoint and the slipped midpoint indicates the overall (average) slip of the detector, *i.e.*, the 'average' *x*- and *y*-displacements of the two detector targets.

This can be calculated by using the distance between the ROIC midpoint and the Detector midpoint after hybridization:

$$\Delta x = \frac{x_{ROIC_{target\,F2}} + x_{ROIC_{target\,F4}} + x_2 + x_4}{2} - \frac{x_{ROIC_{target\,F2}} + x_{ROIC_{target\,F4}}}{2} = \frac{x_2 + x_4}{2}$$

$$\Delta y = \frac{y_{ROIC_{target\,F2}} + y_{ROIC_{target\,F4}} + y_2 + y_4}{2} - \frac{y_{ROIC_{target\,F2}} + y_{ROIC_{target\,F4}}}{2} = \frac{y_2 + y_4}{2}$$

The vector that runs between the two ROIC Targets can be found by subtracting their (nominal) coordinates:

$$\vec{r} = \left\langle x_{ROIC_{target\,F4}} - x_{ROIC_{target\,F2}},\ y_{ROIC_{target\,F4}} - y_{ROIC_{target\,F2}} \right\rangle$$

The vector that runs between the two Detector Targets can be found by subtracting their (slipped) coordinates:

$$\vec{d} = \left\langle (x_{ROIC_{target\,F4}} + x_4) - (x_{ROIC_{target\,F2}} + x_2),\ (y_{ROIC_{target\,F4}} + y_4) - (y_{ROIC_{target\,F2}} + y_2) \right\rangle$$

The angle between the two vectors can be found with the dot product:

$$\theta = \begin{cases} \cos^{-1}\left(\dfrac{\vec{r}\cdot\vec{d}}{\|\vec{r}\|\cdot\|\vec{d}\|} \right), & \text{if } \vec{r}\cdot\vec{d} \geq 0 \\ \cos^{-1}\left(\dfrac{\vec{r}\cdot\vec{d}}{\|\vec{r}\|\cdot\|\vec{d}\|} \right) - \pi, & \text{if } \vec{r}\cdot\vec{d} < 0 \end{cases}$$

The inverse cosine will return a positive angle between 0 and π, so if the dot product is negative, the returned angle will be greater than π/2. This rotation angle would flip the detector around. To avoid this, use the algorithm that if θ > π/2, then just subtract π from θ to give the rotation angle. A positive rotation angle rotates the detector in a counter clockwise sense (when the rotation is viewed from above).

Once the rotation angle θ and the translation (Δx, Δy) have been calculated, the transformation to determine the slipped position (x_{slip}, y_{slip}) of any point (x_{nom}, y_{nom}) in the detector is given by a transformation in two steps: (1) translate the nominal position by (Δx, Δy); then (2) Rotate the translated position about the slipped detector midpoint. These two steps are summarized in the following matrix representation:

$$\begin{bmatrix} x_{slip} \\ y_{slip} \end{bmatrix} = \begin{bmatrix} \cos\theta & \sin\theta \\ -\sin\theta & \cos\theta \end{bmatrix} \cdot \begin{bmatrix} (x_{nom} + \Delta x) - (x_{ROIC_{mid}} + \Delta x) \\ (y_{nom} + \Delta y) - (y_{ROIC_{mid}} + \Delta y) \end{bmatrix} + \begin{bmatrix} (x_{ROIC_{mid}} + \Delta x) \\ (y_{ROIC_{mid}} + \Delta y) \end{bmatrix}$$

$$= \begin{bmatrix} \cos\theta & \sin\theta \\ -\sin\theta & \cos\theta \end{bmatrix} \cdot \begin{bmatrix} x_{nom} - x_{ROIC_{mid}} \\ y_{nom} - y_{ROIC_{mid}} \end{bmatrix} + \begin{bmatrix} (x_{ROIC_{mid}} + \Delta x) \\ (y_{ROIC_{mid}} + \Delta y) \end{bmatrix}$$

The (x, y) location of all reference pixels after hybridization slip is found by applying the transformation to the nominal (x, y) locations of the reference pixels within the ROIC fiducial coordinate system.

This transformation gives the probable (*x, y*) location of reference pixels in the ROIC fiducial coordinate system. To establish the probable *z*-locations, hybrid gap information is required. Figure 3 shows gap data values that are typically recorded at the hybridization step. These values can be used to establish the image plane equation within the ROIC fiducial coordinate system. Four points in the image plane (in ROIC fiducial coordinates) can be found by using the (*x, y*) locations of the hybrid gap measurements, and the corresponding hybrid gap measurements provide the *z*-height at those locations. The best-fit plane through the four points can be calculated, *e.g.*, by Gaussian elimination with maximum pivot scaling [5, 6, 7]. The 'best-fit' plane Normal Vector is given by N = (N_1, N_2, 1), and the 'best-fit' plane equation is

$$N_1 \cdot x + N_2 \cdot y + z = d$$

The normal vector should be made unit length, and the plane equation for the bottom of the detector (*i.e.*, the image plane) becomes

$$\mathrm{N}_{-\mathrm{D}-} = \frac{\langle N_1, N_2, 1 \rangle}{\sqrt{N_1^2 + N_2^2 + 1}}, \quad \mathrm{d}_{-\mathrm{D}-} = \frac{d}{\sqrt{N_1^2 + N_2^2 + 1}}, \quad \mathrm{N}_{\text{-D-}} \cdot \langle x, y, z \rangle = \mathrm{d}_{-\mathrm{D}-}$$

The *z*-values in the plane for any (*x*, *y*) location can be found from the plane equation:

$$z = \frac{\mathrm{d}_{-\mathrm{D}-} - x \cdot \mathrm{N}_{\text{-D-}}(1) - y \cdot \mathrm{N}_{\text{-D-}}(2)}{\mathrm{N}_{\text{-D-}}(3)}$$

The *z*-heights can be calculated at the probable (*x, y*) locations of the reference pixels, giving the probable (*x, y, z*) locations of each reference pixel within the ROIC fiducial coordinate system.

In the context of active alignment, the reference pixel locations are not typically accessible with the aligner-bonder measurement system. However, the FPA fiducials can usually be measured during alignment. The probable (*x, y, z*) locations of reference pixels in the aligner-bonder coordinate system can be calculated from two things: (1) measurements of the FPA fiducials in the aligner-bonder coordinate system; and (2) the fixed spatial relationship between the fiducials and the reference pixels within the ROIC fiducial coordinate system. For example, suppose reference Pixel (1, 1) is at location (x_1, y_1, z_1) within the ROIC fiducial coordinate system (as determined from hybrid slip and gap measurements, and the algorithms above). Further suppose that measurements of three fiducials on the FPA have been made in the aligner-bonder coordinate system, F_1, F_2 and F_3. Then the location of the reference pixel in the aligner-bonder coordinate system can be found from

$$Pixel(1,1) = F_1 + x_1 \cdot \frac{F_3 - F_2}{\|F_3 - F_2\|} + y_1 \cdot \frac{F_2 - F_1}{\|F_2 - F_1\|} + z_1 \cdot \frac{(F_2 - F_1) \times (F_3 - F_2)}{\|(F_2 - F_1) \times (F_3 - F_2)\|}$$

In practice, this transformation can be made more robust to fiducial measurement uncertainty by requiring the second (*y*) direction vector to be perpendicular to the first. Some care must also be taken to ensure that the vertical (*z*) direction vector is pointing upward.

MOUNTING PLATFORM PRE-CHARACTERIZATION

For active alignment, the location of mechanical reference datums must be determined within the aligner-bonder measurement system. However, reference datums are often inaccessible to the aligner-bonder measurement system. In this case, fiducials can be placed on a mounting tool that will be accessible to the aligner-bonder measurement system during alignment. The main idea presented in [5] is that the spatial relationship between the fiducials and reference datums remains

fixed, and that the fixed spatial relationship can be captured mathematically. Pre-characterization measurements and algorithms presented in [5] can accomplish this goal.

Three fiducials are placed on the mounting tool in such a way that they can be viewed by the measurement system during alignment. Datum transfer parameters are calculated from a series of measurements. The datum transfer parameters are stored, and used later to determine datum locations from fiducial measurements during active alignment. Two plane equations (fiducial plane, datum plane) are calculated from the pre-characterization data. The relationship between the two planes can be described mathematically by three 'plane transfer values' representing the distance from the fiducial points to the Datum -A- plane *along the fiducial plane normal vector*. This general approach is depicted in Figure 1 (reproduced from [5, figure 4]). The 'plane transfer values' are then stored for later use when the datum surface is obscured to the measurement system; measurements of the fiducials can be used with the 'plane transfer values' to calculate the datum location.

OPERATIONAL DETERMINATION OF DATUM SURFACES

As depicted in Figure 1, three plane transfer values are calculated from the Datum -A- plane equation and the fiducial plane equation, based on data collected during tool characterization, per [5] equation (10):

$$t_1 = \frac{d_{-A-} - N_{-A-} \cdot F_1}{N_{-A-} \cdot N_{-F-}} = (\pm)\left\| F_1 - FA_1 \right\|_2 \qquad t_2 = \frac{d_{-A-} - N_{-A-} \cdot F_2}{N_{-A-} \cdot N_{-F-}} = (\pm)\left\| F_2 - FA_2 \right\|_2$$

$$t_3 = \frac{d_{-A-} - N_{-A-} \cdot F_3}{N_{-A-} \cdot N_{-F-}} = (\pm)\left\| F_3 - FA_3 \right\|_2$$

The 'plane transfer values', along with measurements of the tool fiducials, can be used during active alignment to establish the datum location within the aligner-bonder coordinate system. The three **virtual points** FA_1, FA_2 and FA_3 in the Datum -A- plane (Figure 1) are calculated from the measured values of F_1, F_2 and F_3 and the fiducial plane equation by using the plane transfer values, and the normal vector to the fiducial plane, per [5] equation (11):

$$FA_1 = F_1 + t_1 * N_{-F-} \qquad FA_2 = F_2 + t_2 * N_{-F-} \qquad FA_3 = F_3 + t_3 * N_{-F-}$$

The Datum -A- plane equation can be calculated from the three virtual points by cross product:

$$N_{-A-} = \left\langle \left\langle FA_2 - FA_1 \right\rangle \times \left\langle FA_3 - FA_1 \right\rangle \right\rangle \cdot \frac{sign\left[\left\langle \left\langle FA_2 - FA_1 \right\rangle \times \left\langle FA_3 - FA_1 \right\rangle \right\rangle (3) \right]}{\left\| \left\langle FA_2 - FA_1 \right\rangle \times \left\langle FA_3 - FA_1 \right\rangle \right\|_2}$$

N_{-A-} is the Datum -A- plane normal vector (unit length, and pointing upward), and the plane equation is

$$N_{-A-} \cdot \langle x, y, z \rangle = N_{-A-} \cdot FA_1$$

where the right-hand side of the equation is the plane d-value ($d_{-A-} = N_{-A-} \cdot FA_1$).

The three virtual points FA_1, FA_2 and FA_3 in Datum -A-, along with additional pre-characterization measurements, can also be used to determine the two other mutually orthogonal datum planes (Datums -B- and -C-). A vector perpendicular to the line from FA_3 to FA_1 (unit length and pointing in the positive y-direction) that is also in the Datum -A- plane is calculated by:

$$FA\_B = \left\langle N_{-A-} \times \left\langle FA_3 - FA_1 \right\rangle \right\rangle \cdot \frac{sign\left[\left\langle N_{-A-} \times \left\langle FA_3 - FA_1 \right\rangle \right\rangle (2)\right]}{\left\| \left\langle N_{-A-} \times \left\langle FA_3 - FA_1 \right\rangle \right\rangle \right\|_2}$$

The 'plane transfer values' for Datum -B- are, per [5], equation 20:

$$t_4 = \frac{d_{-B-} - N_{-B-} \cdot FA_1'}{N_{-B-} \cdot FA\_B} \qquad t_5 = \frac{d_{-B-} - N_{-B-} \cdot FA_3'}{N_{-B-} \cdot FA\_B}$$

The plane transfer values have a magnitude that is equal to the distance between the virtual points FA_1 and FA_3 and the Datum -B- plane, and a sign that depends on the direction of the FA_B vector. During active alignment, two virtual points FB_1 and FB_2 in the Datum -B- plane are calculated using the Datum -B- 'plane transfer values' per [5] equation (28):

$$FB_1 = FA_1 + t_4 * FA\_B \qquad FB_2 = FA_3 + t_5 * FA\_B$$

The Datum -B- normal vector (unit length and pointing in the direction of the positive y-axis) is found by cross product of the vector between the two virtual points with the Datum -A- normal:

$$N_{-B-} = \left\langle N_{-A-} \times \left\langle FB_2 - FB_1 \right\rangle \right\rangle \cdot \frac{sign\ \left[\left\langle N_{-A-} \times \left\langle FB_2 - FB_1 \right\rangle \right\rangle (2)\right]}{\left\| \left\langle N_{-A-} \times \left\langle FB_2 - FB_1 \right\rangle \right\rangle \right\|_2}$$

and the Datum -B- plane equation is

$$N_{-B-} \cdot \langle x, y, z \rangle = N_{-B-} \cdot FB_1$$

where the right-hand side of the equation is the plane d-value ($d_{-B-} = N_{-B-} \cdot FB_1$).

A vector perpendicular to the line from the points FA_2 to FA_1 (unit length and pointing in the positive x-direction) that is also in the Datum -A- plane is calculated by

$$FA\_C = \left\langle N_{-A-} \times \left\langle FA_2 - FA_1 \right\rangle \right\rangle \cdot \frac{sign\left[\left\langle N_{-A-} \times \left\langle FA_2 - FA_1 \right\rangle \right\rangle (1)\right]}{\left\| \left\langle N_{-A-} \times \left\langle FA_2 - FA_1 \right\rangle \right\rangle \right\|_2}$$

The 'plane transfer value' for Datum -C- is, per [5] equation (27):

$$t_6 = \frac{d_{-C-} - N_{-C-} \cdot FA_1''}{N_{-C-} \cdot FA\_C}$$

The plane transfer value has a magnitude that is equal to the distance between the point FA_1 and the Datum -C- plane along the FA_C vector, and a sign that depends on the direction of the FA_C vector. The transfer value t_6 can be used to determine a point in the Datum -C- plane. A vector perpendicular to the line from the points FA_2 to FA_1 (unit length and pointing in the positive x-direction) that is also in the Datum -A- plane is calculated by:

$$FA\_C = \left\langle N_{-A-} \times \left\langle FA_2 - FA_1 \right\rangle \right\rangle \cdot \frac{sign\left[\left\langle N_{-A-} \times \left\langle FA_2 - FA_1 \right\rangle \right\rangle (1)\right]}{\left\| \left\langle N_{-A-} \times \left\langle FA_2 - FA_1 \right\rangle \right\rangle \right\|_2}$$

Then, the virtual point FC_1 in the Datum -C- plane is calculated using the Datum -C- 'plane transfer value', per [5] equation (31):

$$FC_1 = FA_1 + t_6 * FA\_C$$

The Datum -C- normal vector (unit length and pointing in the direction of the positive *x*-axis) is found by cross product of the vector between the two other datum normal vectors:

$$N_{-C-} = \left\langle N_{-A-} \times N_{-B-} \right\rangle \cdot \frac{sign\ \left[\left\langle N_{-A-} \times N_{-B-} \right\rangle (1)\right]}{\left\| \left\langle N_{-A-} \times N_{-B-} \right\rangle \right\|_2}$$

and the Datum -C- plane equation is

$$N_{-C-} \cdot \langle x, y, z \rangle = N_{-C-} \cdot FC_1$$

where the right-hand side of the equation is the plane *d*-value ($d_{-C-} = N_{-C-} \cdot FC_1$).

The origin of the datum coordinate system can be found by solving the plane equations simultaneously. The three datum planes are mutually orthogonal, and the point of intersection of all three planes represents the origin point of the Datum Coordinate System. The three plane equations form a system of three equations in three unknowns, where the solution of the system of equations is the origin point.

$$N_{-A-}(1) \cdot x + N_{-A-}(2) \cdot y + N_{-A-}(3) \cdot z = d_{-A-}$$
$$N_{-B-}(1) \cdot x + N_{-B-}(2) \cdot y + N_{-B-}(3) \cdot z = d_{-B-}$$
$$N_{-C-}(1) \cdot x + N_{-C-}(2) \cdot y + N_{-C-}(3) \cdot z = d_{-C-}$$

The system of equations can be solved, for example, by Gaussian elimination with pivot scaling and back substitution [*e.g.*, 7]. In this case, since the datum planes are all mutually orthogonal and the linear system is well behaved, more efficient methods can be used, *e.g.*, as described in [5].

ALIGNING REFERENCE PIXELS TO DATUM SURFACES

To accomplish a complete FPA alignment, a tip-tilt stage is required, as well as a rotating bond-head (or a rotating portion on the tip-tilt stage). The general alignment process can be summarized in three procedures: (1) measure the FPA fiducials, and determine the current location of reference pixels; (2) measure the mounting tool fiducials, and determine the current location of reference datums; (3) calculate the tip-tilt stage and bond-head motions that will bring the FPA into parallelism and clocking alignment. Motions of the mounting platform and die are always co-dependent, in such a way that any movements that are made to adjust the parallelism alignment will affect clocking, and vice versa. An iterative approach is useful here, where several iterations are performed numerically to arrive at an 'optimal' set of actuator movements that corrects for mis-alignment in both parallelism and clocking at the same time.

For parallelism alignment, a typical system consists of three tip-tilt actuators that drive a kinematic stage beneath the mounting platform (Figure 4). The tip-tilt stage moves to bring the datum plane parallel to the image plane. To determine movements required by each actuator, first determine the rotation axis and rotation angle that will bring the normal vectors into alignment.

$$R_{\langle x,y,z \rangle} = \frac{\left\langle N_{-A-} \times N_{-D-} \right\rangle}{\left\| N_{-A-} \times N_{-D-} \right\|_2}$$ (The rotation axis for aligning to -A-, a (unit length) vector)

$$\theta = \arccos\left[\frac{N_{-A-} \cdot N_{-D-}}{\left\| N_{-A-} \right\|_2 \cdot \left\| N_{-D-} \right\|_2} \right]$$ (The rotation angle for aligning to -A-, a scalar)

The rotation matrix corresponding to the rotation axis and rotation angle is

$$\left[R_{\langle x,y,z\rangle}\right]=\begin{bmatrix} \cos\theta+x^2\cdot(1-\cos\theta) & -z\cdot\sin\theta+x\cdot y\cdot(1-\cos\theta) & y\cdot\sin\theta+x\cdot z\cdot(1-\cos\theta) \\ z\cdot\sin\theta+x\cdot y\cdot(1-\cos\theta) & \cos\theta+y^2\cdot(1-\cos\theta) & -x\cdot\sin\theta+y\cdot z\cdot(1-\cos\theta) \\ -y\cdot\sin\theta+x\cdot z\cdot(1-\cos\theta) & x\cdot\sin\theta+y\cdot z\cdot(1-\cos\theta) & \cos\theta+z^2\cdot(1-\cos\theta) \end{bmatrix}$$

The rotation is applied to the nominal (x, y, z) positions of two tip-tilt actuators, using the third actuator as the origin point of the rotation. The z-difference between the nominal and rotated positions will give the actuator motion required to make the parallelism adjustment (within a tiny cosine error, depending on the footprint of the tip-tilt stage). This adjustment will (almost always) change the current clocking alignment. The bond-head rotation angle is calculated as the angle between the locations of the die reference pixels projected onto the datum plane and the relevant datum clocking feature. It is usually sufficient to assume that the bond-head rotation axis is 'vertical' (if greater precision is required, the rotation axis in datum coordinates can be calculated from successive measurements of the die fiducials before and after a significant rotation). In this case, the angle between die reference pixel projections and the datum clocking feature represents the required actuator motion. This adjustment will (almost always) change the current parallelism alignment. Numerical iterations of parallelism and clocking adjustments can be made until the alignment converges to a specified precision. The final locations of each actuator are then compared to their current positions to establish the required movements to bring the die reference pixels into alignment with the datums.

NOTES ABOUT ACCURACY, PRECISION

The algorithms presented here and in [5] have been successfully implemented for ultra-precision, active manufacturing alignment and post-alignment measurement of infrared imaging systems. Precision depends on encoder resolution. The accuracy of the final alignment depends on the measurement uncertainty of the alignment system (and to some degree on the temperature conditions of the manufacturing environment). The algorithms do not (under normal circumstances) cause small measurement errors to blow up and give erroneous results. Since repeated measurements of the datum surfaces are used, standard statistical techniques can be used to estimate measurement error. The magnitude of alignment uncertainty can be calculated by allowing the measurement uncertainty to propagate through the algorithm calculations. Volumetric calibration of the measurement system is required, and for high-precision alignment, the use of non-linear error correction for all stage axes is essential. Using high-precision encoders, high-quality optics and sufficiently corrected stages, measurement guard bands for alignment errors are significantly better than manufacturing tolerances for FPA mounting platforms.

REFERENCES

1. Shin, Lloyd and Gregory S. Winters, 1993, NICMOS flight focal plane assembly, *in* Bely, Pierre Y. and James B. Breckinridge, Editors, Astronomical Telescopes and Instruments II, Proceedings of SPIE, Volume 1945, pp.371-382, ISBN 0-8194-1181-7.
2. Yokoyama, Karen E., Harold Miller, Jr., Ted Hedman, Sveinn Thordarson, Miguel Figueroa, John Shepanski, Peter J. Jarecke and Steven Lai, 2003, NGST longwave hyperspectral imaging spectrometer system characterization and calibration, in Shen, Sylvia S. and Paul E.

Lewis, Editors, Imaging Spectrometry IX, Proceedings of SPIE, Volume 5159, pp. 262-274, ISBN 0-8194-5032-4
3. Stone, Jack A., Mohamed Amer, Bryon Faust and Jay Zimmerman, 2004, Uncertainties in small-angle measurement systems used to calibrate angle artifacts, Journal of Research of the National Institute of Standards and Technology, Volume 109, No. 3, May-June 2004 Issue, pp. 319-333.
4. Lehmann, Peter, 2003, Optical versus tactile geometry measurement: alternatives or counterparts, *in* Osten, Wolfgang, Malgorzata Kujawinska and Katherine Creath, Editors, Optical Measurement Systems for Industrial Inspection III, Proceedings of SPIE, Volume 5144, , May 2003, pp. 183-196, ISBN 0-8194-5014-6.
5. Hughes, Gary, 2006, Algorithms for Sensor Chip Alignment to Blind Datums, Journal of Electronic Imaging, in press.
6. Spaeth, Helmut, 1991, Mathematical Algorithms for Linear Regression, Elsevier Academic Press, San Diego, CA, 327 pages, ISBN 0-12-656460-4
7. Press, William H., Saul A. Teukolsky, William T. Vetterling and Brian P. Flannery, 1992. Numerical Recipes in C, The Art of Scientific Computing, Second Edition. Cambridge University Press, New York, NY, 994 pages, ISBN 0-521-43108-5.

FIGURES

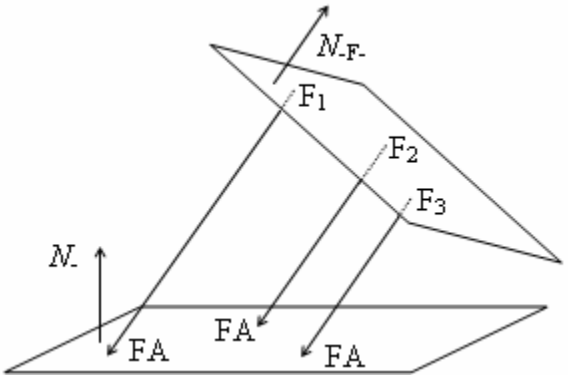

Figure 1. 'Plane transfer values' are scalars that denote distances from fiducial locations to virtual points on the (blind) datum planes (or detector active plane) along vectors determined by the fiducial locations. In a manufacturing context, the fiducials can be measured during the alignment process, but the datum surfaces cannot. The 'plane transfer values' are determined during a pre-characterization, and used during alignment to determine datum plane locations. In this figure, the points F_1, F_2 and F_3 are fiducial marks that can be measured during manufacturing alignment. The 'plane transfer values' denote the distances from the fiducial marks to the virtual points FA_1, FA_2 and FA_3 on the Datum plane. The distances are in the direction of the fiducial plane normal vector N_{F-}. The Datum plane equation is then calculated from the three virtual points. The central idea of this method is that the spatial relationship between the fiducials and datums does not change when spatial orientation of the rigid body changes.

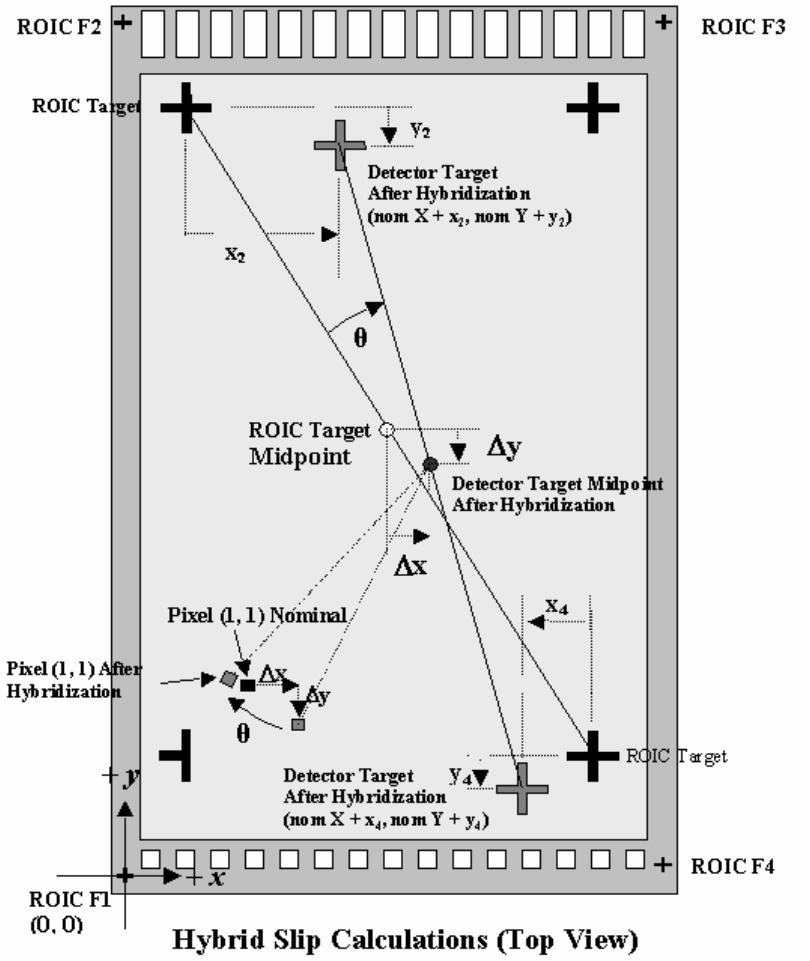

Figure 2. Hybridization Slip Measurements and Calculations. The slips are exaggerated for clarity of the illustration. Measurements of hybrid slip are typically made with an IR microscope, and record the offset of detector fiducials with respect to the ROIC Hybridization targets. In order to determine the overall effect of hybridization slip, measurements of the individual targets must be combined to establish an overall movement for the entire detector. The figure shows measurements in the ROIC coordinate system. Care must be taken to interpret data from individual targets in the context of this coordinate system. Hybridization slip is characterized as the movement of the Detector Target relative to the ROIC. The relative motions are applied to the nominal locations of the ROIC targets to give the absolute positions of the slipped Detector targets in the ROIC coordinate system. To determine the resulting location of Pixel (1, 1), hybridization slip movements can be summarized by one translation (Dx, Dy) and one rotation through an angle θ about the midpoint of the line segment joining the detector targets. The resulting positions are calculated by applying the translation and rotation to the nominal locations in the ROIC coordinate system.

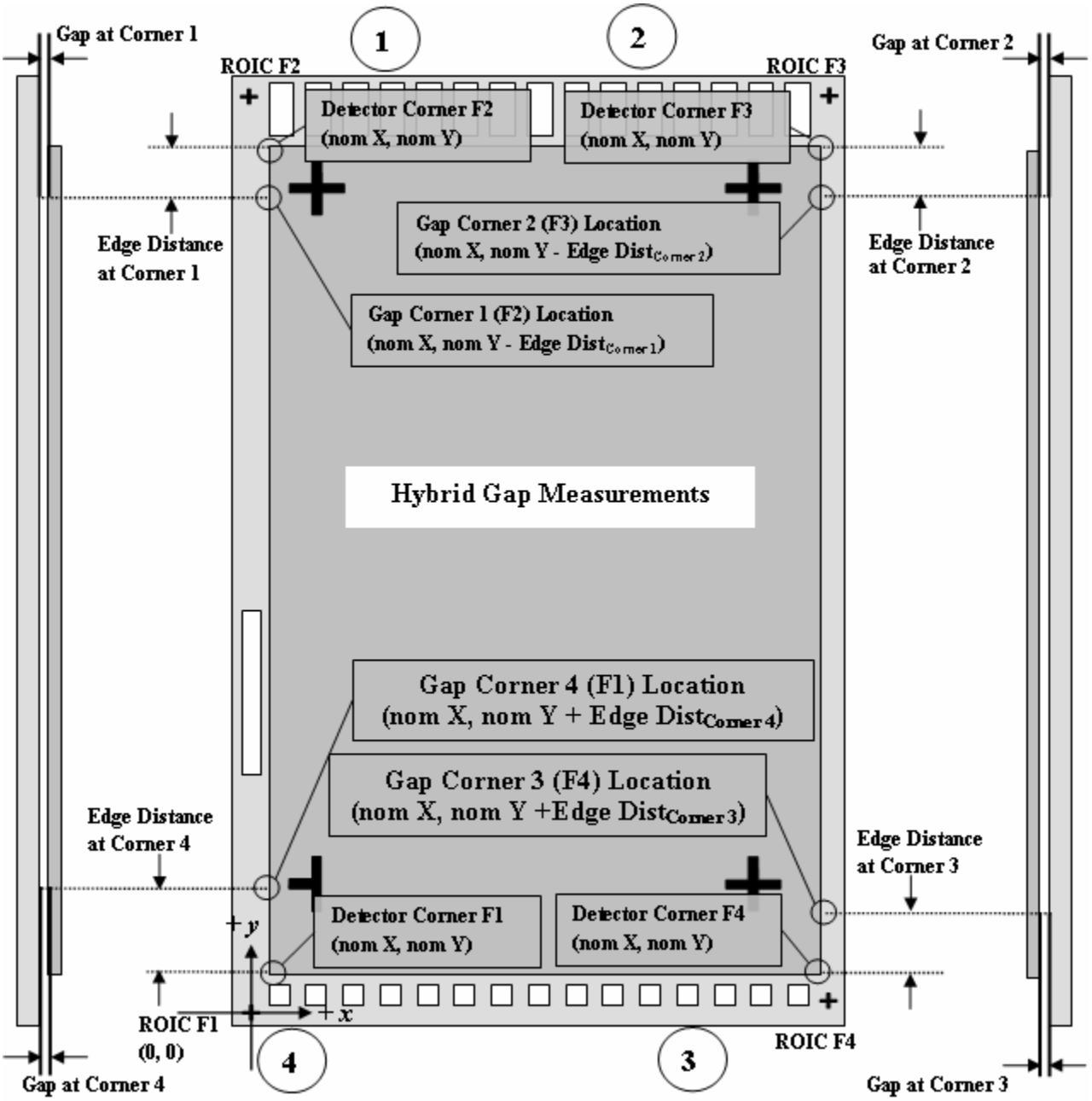

Figure 3. Hybridization Gap Measurements. Each gap measurement is made along the edge of the Detector near the corner, including an edge distance from the detector corner where the gap measurement was made. The edge distance is added to the nominal detector corner location *y*-value to give the (*x*, *y*) location of the gap measurement in the ROIC coordinate system. Gap measurements are then used to determine the image plane equation. The plane equation determined from hybrid slip and gap measurements is used to determine the (*x*, *y*, *z*) location of reference pixels.

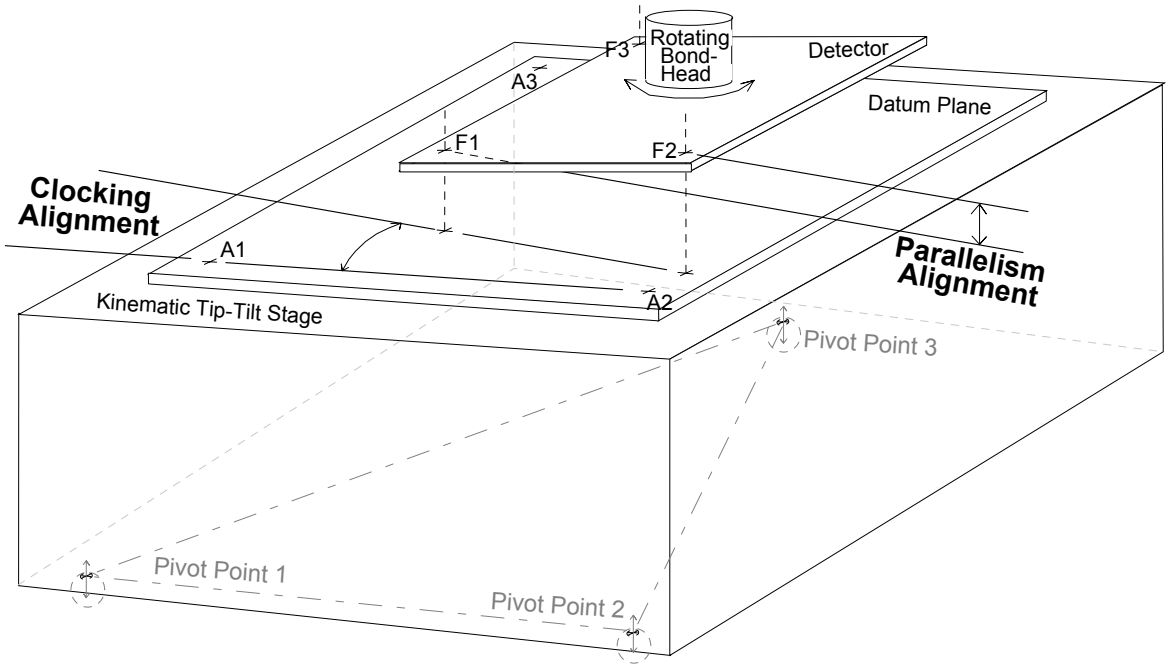

Figure 4. Representation of a common alignment scheme using a kinematic tip-tilt stage. The stage pivots are moved up or down to bring the datum surface into parallelism alignment with the detector image plane. This motion also affects clocking, so some mechanism is also required for rotating the detector relative to the datums. A common approach is to mount the detector in a rotating bond head. The tip-tilt stage moves in *x*- and *y*-directions underneath the detector, and the bond head moves up and down (in *z*).